

# Development of structural debris flow fragility curves (debris flow buildings resistance) using momentum flux rate as a hazard parameter

Jorge A. Prieto<sup>a,\*</sup>, Murray Journey<sup>b</sup>, Ana B. Acevedo<sup>a</sup>, Juan D. Arbelaez<sup>a</sup>, Malaika Ulmi<sup>b</sup>

<sup>a</sup> EAFIT University, Carrera 49 7 Sur-50, Avenida Las Vegas, Bloque, 19-647 Medellín, Colombia

<sup>b</sup> Natural Resources Canada, 1500-605, Robson St., Vancouver, BC V6B 5J3, Canada

## ARTICLE INFO

### Keywords:

Debris flow fragility curves  
Debris flow vulnerability  
Debris flow hazard  
Debris flow losses  
Debris flow risk  
Debris flow building resistance

## ABSTRACT

Societal risks associated with debris flow hazards are significant and likely to escalate due to global population growth trends and the compounding effects of climate change. Quantitative risk assessment methods (QRA) provide a means of anticipating the likely impacts and consequences of settlement in areas susceptible to landslide activity and are increasingly being used to inform land use decisions that seek to increase disaster resilience through mitigation and/or adaptation. Current QRA methods for debris flow hazards are based primarily on empirical vulnerability functions that relate hazard intensity (depth, velocity, etc.) to expected levels of loss for a given asset of concern, i.e. most of current methods are dedicated to loss-intensity relations. Though grounded in observed cause-effect relationships, empirical vulnerability functions are not designed to predict the capacity of a building to withstand the physical impacts of a debris flow event, or the related uncertainties associated with modelling building performance as a function of variable debris flow parameters. This paper describes a methodology for developing functions that relate hazard intensity to probability of structural damage, i.e., fragility functions, rather than vulnerability functions, based on the combined hydrodynamic forces of a debris flow event (*hazard level*) and the inherent structural resistance of building typologies that are common in rural mountainous settings (*building performance*).

Hazard level includes a hydrodynamic force variable ( $F_{DF}$ ), which accounts for the combined effects of debris flow depth and velocity, i.e. momentum flux ( $h v^2$ ), material density ( $\rho$ ) and related flow characteristics including drag ( $C_d$ ) and impact coefficient ( $K_d$ ). Building performance is measured in terms of yield strength ( $A_y$ ), ultimate lateral capacity ( $A_U$ ) and weight to breadth ratios ( $W/B$ ) defined for a portfolio building types that are common in mountain settlements. Collectively, these model parameters are combined using probabilistic methods to produce building-specific fragility functions that describe the probability of reaching or exceeding successive thresholds of structural damage over a range of hazard intensity values, expressed in terms of momentum flux. Validation of the proposed fragility model is based on a comparison between model outputs and observed cause-effect relationships for recent debris flow events in South Korea and in Colombia. Debris flow impact momentum fluxes, capable of resulting in complete damage to unreinforced masonry buildings (URM) in those regions are estimated to be on the order of  $24 \text{ m}^3/\text{s}^2$ , consistent with field-based observations. Results of our study offer additional capabilities for assessing risks associated with urban growth and development in areas exposed to debris flow hazards.

## 1. Introduction

Debris flows produce significant social and economic losses worldwide. A global study of 213 debris flow events documented 77,779 fatalities over a 60-year period from 1950 to 2011 (Dowling and Santi, 2014). The global economic consequences of hydrologic hazards increased from 39% to 50% during 2016 (relative to the previous 35 years) with losses on the order of US\$ 56 billion in the same year, while cumulative losses over the period from 1980 to 2015 are

estimated to be more than US\$ 954 billion (Munich Re, 2017). Debris flow events represent a significant portion of this trend and can be catastrophic in mountainous regions, where human settlement and its associated infrastructure development are often localized in valley bottoms. A recent large-scale debris flow event in April of 2017 partially buried the city of Mocoa in southwest Colombia resulting in over 250 fatalities, including 70 children (INMLCF, 2017). More localized debris flow events can also cause grievous socioeconomic losses (Jakob et al., 2012; Totschnig and Fuchs, 2013). The frequency and

\* Corresponding author.

E-mail addresses: [jprieto7@eafit.edu.co](mailto:jprieto7@eafit.edu.co) (J.A. Prieto), [murray.journey@canada.ca](mailto:murray.journey@canada.ca) (M. Journey), [aaceved14@eafit.edu.co](mailto:aaceved14@eafit.edu.co) (A.B. Acevedo), [malaika.ulmi@canada.ca](mailto:malaika.ulmi@canada.ca) (M. Ulmi).

<https://doi.org/10.1016/j.enggeo.2018.03.014>

Received 23 November 2017; Received in revised form 17 March 2018; Accepted 17 March 2018

Available online 23 March 2018

0013-7952/ © 2018 Elsevier B.V. All rights reserved.

socioeconomic consequences of similar catastrophic debris flow events are likely to escalate with increased population growth and the compounding effects of climate change.

Quantitative risk assessment methods are increasingly being used to estimate the socioeconomic consequences of debris flow hazards (e.g. Jakob et al., 2012; Papathoma-Köhle et al., 2012; Totschnig and Fuchs, 2013; Kang and Kim, 2016). Most of this research (see Table 1) is focused on the development of empirical vulnerability functions that express a relationship between economic losses and a hazard intensity parameter (loss-intensity relation); a reduced number of authors are focused on fragility functions (probability of damage-intensity relations). Though grounded in observed cause-effect relationships, empirical vulnerability functions are not designed to predict the capacity of a building to withstand the physical impacts of a mass flow event, or the related uncertainties associated with modelling building performance as a function of variable debris flow parameters. A more rigorous analytic approach involves the development of fragility functions that model the probability of exceeding a damage state threshold for a given hazard intensity parameter such as flow depth and/or velocity (damage-intensity function). Damage state probabilities provide the necessary foundation for estimating related socioeconomic consequences and can be used in conjunction with empirical loss data to derive quantitative debris flow risk models.

There are several key advantages to using process-based fragility models for assessing the likely impacts and consequences of debris flow events. The estimation of expected casualties in and around buildings depends primarily on the level of structural damage sustained, not just on the hazard intensity of the debris flow event. Fragility functions provide a means of modelling cause-effect relationships between the physical forces of a debris flow event and the structural resistance of common building typologies. As a result, they can be used to model debris flow risks for existing and potential new buildings. This tool supports both land use planning and the development of performance-based engineering guidelines for the design and construction of disaster resilience buildings (FEMA, 2012). By definition, fragility functions provide a measure of uncertainty associated with modelling the structural resistance of buildings exposed to the hydrodynamic forces of a debris flow event. Direct assessment of damage state probabilities for a range of intensity values allows debris flow fragility functions to be combined with those developed for related threats of concern (floods, earthquakes, etc.), thereby providing the necessary mathematical foundation for modelling multi-hazard risks at local and regional scales.

It is worth noting that certain hazard intensity parameters, such as combinations of flow depth and velocity, maintain consistent relationships with building damage regardless of the scale of the debris flow. For example, the product of flow depth and the square of velocity, i.e. momentum flux ( $hV^2$ ) has been observed to be consistent with the building damage using 68 events worldwide on a scale from 100 m<sup>3</sup> to 10 million m<sup>3</sup>, Jakob et al. (2012).

This paper describes a methodology for developing fragility functions based on the combined hydrodynamic forces of a debris flow event (hazard potential) and the inherent structural resistance of common building typologies (building performance). Hazard potential accounts for the effects of debris flow momentum flux ( $hV^2$ ), density of the flow material ( $\rho$ ), a basal drag coefficient ( $C_d$ ), and an impact coefficient ( $K_d$ ). Building performance is measured in terms of yield strength ( $A_y$ ), ultimate lateral capacity ( $A_U$ ), and the weight to breadth ratio ( $W/B$ ) for a portfolio of common building types. Collectively, these model parameters are combined using probabilistic methods to produce building-specific fragility functions that use momentum flux as the input parameter. Validation of the proposed fragility model is based on a comparison between model outputs and observed cause-effect relationships for debris flow events in South Korea and in Colombia, which affected unreinforced masonry buildings (URM buildings).

## 2. Debris flow modelling and vulnerability: previous work

A complete solution to the problem of structural damage to buildings due to debris flow forces involves the understanding of the physical interaction between debris flow forces and buildings, a complex task, both theoretically and experimentally. Advances on debris flow modelling have been developed mainly from the geoscience side, while improvements on understanding damage to buildings, i.e. vulnerability and fragility aspects, have usually been achieved on structural engineering grounds. Therefore, before introducing the proposed method, aspects of debris flow physical modelling are briefly mentioned as well as elements of building fragility.

Reviews of debris flow physics and models are available in Takahashi (1991), Hutter et al. (1996), Iverson (1997), Iverson and Denlinger (2001), Hungr and McDougall (2009), Takahashi (2009). Modelling of debris flow involves solving equations that represent fundamental physics laws, e.g. conservation of mass and energy, Newton's second law (of linear momentum), or the second law of thermodynamics, subject to given boundary and initial conditions, to obtain problem unknowns such as velocity, debris flow height, water pressures, stresses, forces, etc. Additionally, constitutive relations like the mechanism for energy dissipation, friction, strength criteria, etc. for different types of media are considered. The nature of the model depends on the assumptions, the simplifications, and the method selected for solving the equations. The debris flow medium can, in general, be modelled either as a single component phase (e.g. either fluid or a fluid-solid mixture), or a two component phase (solid and fluid). The fluid part can be plain water or a mix of highly concentrated fine sediment and water slurry, while the solid fraction represents coarse particles. Two component phase models are characterized by the coarse grain (solid) concentration by volume, among other parameters. The model domain can be either in 3, 2 or 1 dimensions. The debris flow bed can be assumed to be either eroded by dynamic action of shear stresses (particles entrainment), or subjected to deposition. External supply or drainage of water can be added to the model. Regarding methods of solutions for the equations, numerical approaches are either continuum mechanics formulations or discrete approaches. A main characteristic to consider is the fact that boundaries are free, i.e. the boundary geometry is changing and must be determined during the solution (e.g. at debris flow fan). When, for analyses, fixed points of the domain are selected and its behaviour is studied as time passes, it is said that the model is using a Eulerian approach. On the other hand, when particles are selected and they are followed as they move and their positions change as function of time, a Lagrangian approach is being employed. When the model domain is reduced from 3 to 2 or 1 D, and some of the field variables are averaged through the cross section or depth, the model is called a hydraulic one. Different constitutive relations, including rheology, are applied to each model. This may include relationships between flow velocity and shear stresses, pore water pressure variation, shear stress failure criteria, etc. To illustrate the assumptions and simplifications used, two examples of main, general, characteristics of models are presented in Table 2, i.e. Takahashi (2009) and Cascini et al. (2016)-Pastor et al. (2015).

It is well known that structural damage to buildings is related directly to the amount of displacement (drift) caused by the lateral forces associated with a geological hazard, (Kircher et al., 1997; Freeman, 1998). Quantitative risk models require expressions that relate an intensity measure of the hazard, or of the amount of structural displacement caused by a hazard and a consequence of it, i.e. damage or loss. These expressions are either vulnerability (intensity-loss relations) or fragility functions (intensity-probability of damage functions). A review of state of the art of these type of expressions is provided in Table 1, from which is clear that most of past research has been dedicated to vulnerability rather than to fragility functions, as was stated before.

Fragility functions provide a means of describing relationships

**Table 1**  
Summary of empirical vulnerability or fragility models used for assessing impacts and consequences of debris flow hazards.

Researchers reference	Input (hazard) parameters	Type of function	Model output	Building typology
Borier (1999)	Combinations of flow depth and velocity, grouped in 3 intensity levels	Step function	Vulnerability, degree of loss from 0 to 1	Generic buildings, Europe
Fuchs et al. (2007)	Deposition height	2nd order polynomial	Vulnerability, degree of loss from 0 to 1	Generic, masonry and concrete, Europe
Haugen and Kaynia (2008)	Sum of hydro static pressure effect and maximum shock displacement	Log-normal Earthquake- fragility functions based on HAZUS building types	Fragility, probability of exceeding damage	Specific to building type, Europe
Akbas et al. (2009)	Deposition height	2nd order polynomial	Vulnerability, degree of loss from 0 to 1	Generic, masonry and concrete, Europe
Calvo and Savi (2009)	Simultaneously velocity and flow depth	bivariate bi-linear function	Vulnerability, degree of loss from 0 to 1	Reinforced concrete, 2-storey residential, Europe
Tsao et al. (2010)	Flow depth	2nd order polynomial	Vulnerability, degree of loss from 0 to 100	Generic masonry and concrete, wooden and sheet metal, Taiwan
Toitschnig et al. (2011)	Deposition height, Ratio deposition height vs building height	Weibull, Frechete, distributions	Vulnerability, degree of loss from 0 to 1	Generic private residential and tourist accommodation, Europe
Quan Luna et al. (2011)	Flow depth, impact pressure and kinematic viscosity	Logistic functions	Vulnerability, degree of loss from 0 to 1	Generic masonry and concrete, 1 to 3-storey, Europe
Lo et al. (2012)	Deposition height	Third order polynomial, bounded	Vulnerability, degree of loss from 0 to 1	Reinforced and unreinforced buildings, Taiwan
Jakob et al. (2012)	Momentum rate flux = flow depth $\times$ velocity <sup>2</sup>	Step function, expressed as a 4 row probability matrix (one row for each damage state)	Probabilities of being in each of four damage states (some sedimentation to complete damage)	Generic, masonry and concrete, world wide database
Papathoma-Kohle et al. (2012)	Deposition height	Weibull distribution	Vulnerability, degree of loss from 0 to 1	Generic, masonry and concrete, Europe
Toitschnig and Fuchs (2013)	Deposition height, Ratio deposition height vs building height	Weibull, log-logistic distributions	Vulnerability, degree of loss from 0 to 1	Generic private residential and tourist accommodation, Europe
Kang and Kim (2016)	Flow depth, velocity, impact pressure	Sigmoid, S-shaped	Vulnerability, degree of loss from 0 to 1	Specific to building type, HAZUS system, Korea
Zhang et al. (2016)	Momentum, Impact force, bending moment	Linear function	Vulnerability, degree of loss from 0 to 1	Brick and concrete walls, China

**Table 2**  
Examples of two debris flow models main characteristics.

Model characteristic	Takahashi (2009)	Cascini et al. (2016)-Pastor et al. (2015)
Domain	2 Dimensions	3 Dimensions reduced to 2 D
Formulation	Eulerian	Lagrangian
Medium	Continuum	Discretized, mesh free using Smoothed Particle Hydrodynamics, SPH
Constitutive relations	Mohr-Coulomb and dilatant fluid	Mohr-Coulomb and viscoplasticity
Comments	Debris flow generated by bed erosion. No specific inclusion of the interaction with barriers, e.g. buildings.	General fast landslides. Inclusion of pore water pressure changes due to consolidation. No specific inclusion of the interaction with barriers, e.g. buildings.

between hazard parameters and damage states, including corresponding uncertainties associated with modelling complex cause-effect relationships. Methods used in this study to develop structural fragility functions for debris flow hazards are analogous to those used for modelling the physical impacts of tsunami hazards in the updated HAZUS 4.0 loss estimation methodology (FEMA, 2017). Relations between the combined hydrodynamic forces of the hazard event and expected levels of lateral displacement for common building typologies are used in conjunction with engineering models of building capacity (strength) to predict damage state thresholds for a range of hazard intensity values. Capacity functions that relate lateral building displacement to physical forces and associated levels of building damage are represented using pushover curves. These capacity-demand relationships are used to derive corresponding fragility functions for representative building typologies that describe the probability of reaching or exceeding specific thresholds of structural damage over a range of hazard intensity values.

A pushover curve, Fig. 1A, is a representation of lateral forces applied to a building ( $F_y$ ) versus its corresponding lateral displacements ( $d_y$ ). The yield capacity ( $F_y$ ,  $d_y$ ) is the point on the curve at which permanent lateral displacement of a building starts, resulting in the permanent deformation of the building. The ultimate capacity ( $F_u$ ,  $d_u$ ) represents the point where structural failure and/or collapse is likely to occur. Both points, yield and ultimate, have uncertainty, and therefore they can be expressed in a probabilistic way. It is worth noting that, in a general form, the vertical axis of a pushover curve can be represented using fractions of the acceleration of gravity instead of forces.

Fragility functions (Fig. 1B) describe the probability of exceeding a specific damage state threshold, e.g. slight, moderate, extensive, complete, over a range of hazard intensity values for a given building typology. Relationships between damage state thresholds and hazard intensity can be established through laboratory tests, engineering analyses and/or expert judgement rooted in field-based studies of

historic landslide events. The methodology described in this study adopts an engineering-based approach that utilizes building capacity functions to derive relationships between debris flow hazard intensity and the probability of sustaining different levels of structural damage. The methodology is informed by and validated using insights on cause-effect relationships from well-documented events that include detailed information on both debris flow hazard intensity and building response characteristics.

### 3. A fragility model for debris flow hazards

There is little consensus on which physical parameters best describe the intensity of a debris flow event for purposes of assessing risks to people and critical assets (See Table 1). Some models use debris flow deposition height, while others use various combinations of flow velocity, building height and debris flow depth. Haugen and Kaynia (2008) combined the hydrostatic pressure effect, i.e. flow depth, and the dynamic effect, i.e. velocity, to develop the concept of debris flow impact force as a process-based measure of hazard intensity. The concept was made operational by Jakob et al. (2012) who compiled a database of 68 debris flow events to derive a hazard intensity index ( $I_{DF}$ ) based on the product of maximum expected flow depth and the square of the maximum flow velocity ( $I_{DF} = hv^2$ ). The impact index is a reasonable proxy for estimating the hydrodynamic action of a debris flow event as it based in classical mechanical theory and represents the flux of force per unit mass (i.e. momentum flux).

Fragility functions developed as part of this study build on the concept of momentum flux to describe hazard intensity of a debris flow event (Jakob et al., 2012) and introduce additional variables that account for variations in flow characteristics and impact potential. The combined lateral hydrodynamic debris flow force ( $F_{DF}$ ) acting on a building can be expressed as (FEMA, 2008, 2017):

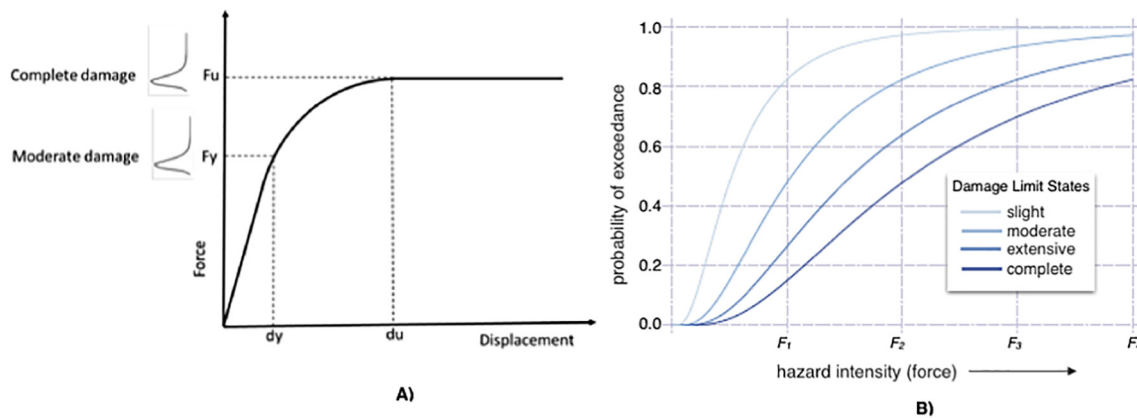


**Fig. 1.** A) Building capacity (pushover) curve.  $F_y$  is the yield capacity (strength, force units),  $F_u$  is the ultimate capacity (force units),  $d_y$  and  $d_u$  (Length units) are the corresponding displacements. Note that both  $F_y$  and  $F_u$  are considered to be random variables (probability density functions plotted in the Figure, vertical axis) that define moderate and complete damage respectively. Extensive damage is defined in the middle between moderate and complete damage. Modified from FEMA (2017). B) Fragility curves describing the probability of reaching or exceeding specified damage state thresholds as a function of lateral forces exerted by a hazard event (intensity).

$$F_{DF} = K_d (0.5 \rho C_d B (hv^2)), \quad (1)$$

where  $K_d$  is a non-dimensional debris impact coefficient,  $\rho$  is the density of the debris flow material,  $C_d$  is a dimensionless drag coefficient,  $B$  is the building breadth, measured normal to flow direction, and  $hv^2$  is the momentum flux, defined as the product of flow depth and the square of maximum flow velocity (Jakob et al., 2012). Note that, in terms of debris flow modelling, Eq. (1) can be interpreted as a 1D averaged force, representative from a debris flow hydraulic model, calculated at the site of impact on a building.

Following methods used to develop the HAZUS tsunami model (FEMA, 2017), we establish a relationship between debris flow force ( $F_{DF}$ ) and lateral building capacity (strength) using pushover curves developed for construction types that are common in rural mountainous settings. The tsunami model (FEMA, 2017) uses HAZUS Earthquake Model to define the strength of building types in terms of seismic design parameters. The lateral capacity of a building (Fig. 1A) is given by.

$$F_y = \alpha_1 A_y W \quad (2)$$

$$F_U = \alpha_1 A_U W \quad (3)$$

where  $F_y$  is the initial yield force at base of building,  $F_U$  is the ultimate capacity force at base of building,  $\alpha_1$  is the dimensionless modal mass parameter,  $W$  is the building weight, and  $A_y$  and  $A_U$  are the fractions of the acceleration of gravity,  $g$ , corresponding to the yield and ultimate capacity forces (note that they are non-dimensional, but can be noted in  $g$  units). Yield and ultimate capacities are related through a unit-less  $\lambda$  parameter thus:

$$A_y = \frac{A_U}{\lambda} \quad (4)$$

Default capacity parameters are based on those defined in the HAZUS methodology for common building typologies (FEMA, 2012). Although structural damage is directly related to the amount of lateral building displacement, it is also possible to relate expected levels of damage to the corresponding physical force of a debris flow event using capacity (pushover) curves for common building archetypes (Fig. 1A). As the hydrodynamic forces associated with a debris flow event are significant, sequential damage states are characterized in terms of complete, extensive or moderate damage thresholds. Complete damage describes situations in which structural failure of the building has occurred, most likely leading to collapse. Extensive damage describes situations in which structural integrity of the building has been compromised but can be restored with extensive repairs. Moderate damage describes situations in which some supporting structural elements of a building are permanently deformed but repairable.

The relationship between lateral capacity and damage state probability is similar to that defined in the HAZUS tsunami model and is based on hazard intensity (hydrologic force) rather than structural displacement (FEMA, 2017). Complete damage to a structure occurs when the debris flow force is equal to the ultimate yield capacity ( $F_U$ ) for a given building type of interest (Fig. 1). Extensive structural damage occurs when the debris flow force is equal to the average value of the yield and ultimate capacity parameters combined ( $F_y + F_U/2$ ). Moderate structural damage occurs when the debris flow force is equal to the yield capacity ( $F_y$ ) for a given building type of interest.

Based on these relationships, debris flow force (Eq. (1)) can be combined with lateral building capacity functions (Eqs. (2), (3) and (4)) to solve for the momentum flux term ( $hv^2$ ) for each damage state threshold:

Complete damage

$$hv_c^2 = \frac{2\alpha_1 A_U W}{K_d \rho C_d B} = \frac{2\alpha_1 A_y \lambda W}{K_d \rho C_d B} \quad (5)$$

Extensive damage

$$hv_e^2 = \frac{\alpha_1 (A_y + A_U) W}{K_d \rho C_d B} = \frac{\alpha_1 A_y (\lambda + 1) W}{K_d \rho C_d B} = \frac{\alpha_1 A_U (\lambda + 1) W}{K_d \rho C_d \lambda B} \quad (6)$$

Moderate damage

$$hv_m^2 = \frac{2\alpha_1 A_y W}{K_d \rho C_d B} = \frac{2\alpha_1 A_U W}{K_d \rho C_d \lambda B} \quad (7)$$

The momentum flux corresponding to each damage state threshold ( $hv_c^2$ ,  $hv_e^2$  and  $hv_m^2$ ) is defined in terms of engineering variables describing the yield or ultimate capacities of a given building ( $A_y$  or  $A_U$ ) and related modal parameters ( $\alpha_1$  and  $\lambda$ ); by structural variables that depend on physical characteristics of buildings impacted by the hazard event including overall weight ( $W$ ) and plan dimensions measured normal to debris flow direction, building breadth ( $B$ ), and; by geologic variables including density of the debris flow material ( $\rho$ ) and characteristics of drag ( $C_d$ ) and impact potential ( $K_d$ ).

Random variables in the model are evaluated using probability density functions and corresponding cumulative distribution functions that represent the combined probability over a given range of values. Cumulative distribution functions are used to define debris flow fragility curves that describe relationships between momentum flux ( $hv^2$ ) and probability thresholds for each of the reference damage states. A common practice in structural engineering and quantitative risk analysis is to use lognormal distribution functions to define fragility thresholds in terms of a median value that represents system behaviour, and a standard deviation value ( $\beta$ ) that represents associated levels of model uncertainty (Porter, 2017). Fragility curves developed as part of this study are defined for sequential damage states using lognormal distribution functions based on Eqs. (5), (6) and (7).

### 3.1. Hazard intensity parameters

This section describes components of the debris flow fragility model that represent overall structural demand (lateral force) in terms of momentum flux ( $hv^2$ ), debris flow density ( $\rho$ ), drag ( $C_d$ ) and impact force potential ( $K_d$ ).

#### 3.1.1. Momentum flux ( $hv^2$ )

Momentum flux is increasingly being used as a hazard intensity parameter for tsunami modelling as it reflects the combined effects of both water depth and flow velocity (Park and Cox, 2016; FEMA, 2017). It is defined mathematically as the product of water depth and the square of maximum flow velocity at a given point ( $hv^2$ ), and is a realistic proxy for hydrodynamic forces that result in lateral displacement to buildings and other assets of concern. The concept of momentum flux is equally applicable to assessing the intensity of debris flow hazards as parameters of depth and flow velocity are often cited in forensic field studies and can be generated using process-based analytic models.

#### 3.1.2. Debris flow density ( $\rho$ )

The density of debris flow material ( $\rho$ ) is considered a random variable represented by a lognormal distribution function with a mean value of 2000 kg/m<sup>3</sup> (Iverson and Denlinger, 2001; Denlinger and Iverson, 2001; Iverson, 2005). This mean value is also used for analysis of events in Korea, (Kang and Kim, 2016). Regarding the uncertainty of the parameter, represented by the standard deviation of natural log,  $\sigma_{\ln}(\rho)$ , Jones et al. (2002) suggest using a value of 0.09. Iverson (1997) mentions that the density of the mixture is usually between 1800 kg/m<sup>3</sup> and 2400 kg/m<sup>3</sup>. Therefore, assuming that 95% of the values are within these two boundaries, a  $\sigma_{\ln}(\rho)$  of 0.12 is obtained, which is selected for the model.

#### 3.1.3. Drag coefficient, $C_d$

A drag coefficient ( $C_d$ ) is used in the model to represent the drag effect between the debris flow and the structure. It is linked to Reynolds number and structure geometry, and assumed to be variable within the

range (1–2.1) with a mean value of 2.0 (Shames, 1992; FEMA, 2008; Cadavid 2017, personal communication). Considering that 95% of the values are within these two boundaries, and using a lognormal distribution, the standard deviation of the natural log of the drag coefficient,  $\sigma_{\ln(C_d)}$  is estimated to be 0.37. It is worth mentioning that for the case of tsunamis, the mean value of the drag coefficient is taken as 2.0 (FEMA, 2017; Kircher, 2012a, 2012b). It will be seen in the model validation section, that this value of the drag coefficient produces consistent results in modelling debris flow hazards.

### 3.1.4. Debris impact force coefficient, $K_d$

The impact coefficient,  $K_d$  represents the lateral forces caused by the presence of material entrained within a debris flow with a potential to cause building damage (coarse size particles, large boulders, etc.).  $K_d$  values are considered to have a mean value of 1.2, with values as high as 2.0 and as low as 0.7, as in the case of tsunamis, FEMA (2017). Assuming that 95% of the values are included within the range mentioned, a standard deviation of the natural logarithm,  $\sigma_{\ln(K_d)}$ , of 0.52, is obtained. These values are consistent with those deduced from field observations, as will be seen later.

## 3.2. Performance parameters

This section describes components of the debris flow fragility model that represent the inherent structural resistance of buildings to debris flow hazards in terms of physical characteristics including weight to breadth ratio ( $W/B$ ), structural yield ( $A_y$ ) and/or ultimate lateral capacity ( $A_U$ ), and associated model parameters ( $\alpha_1$ , and  $\lambda$ ).

### 3.2.1. Weight to breadth ratio $W/B$

Weight and breadth parameters can be statically correlated as it will be shown below. Therefore, we decided using the ratio  $W/B$  as a model parameter rather than the two of them independently. These ratios were derived using statistical correlations between variables reported for a portfolio of unreinforced masonry (URM) buildings in Colombia and for representative HAZUS building taxonomies that are common in remote mountainous terrain. We used data collected from 40 URM buildings of 1 to 4 stories in the city of Medellin, Antioquia province, Colombia. The subset of data was compiled from a regional study of vulnerability for the South American Risk Assessment project (SARA), a collaborative research partnership with the Global Earthquake Model foundation (GEM). Details of this study are reported by Acevedo et al. (2016).

Nearly 70% of all buildings in the metropolitan area of Medellin are of unreinforced masonry construction (URM). Most of them were built between 1958 and 1998. Roofs and floors are made either of concrete, asbestos-cement mix or clay tiles. Structural and geometrical characteristics of the buildings were obtained after field visits. The distribution of  $W$  and  $B$  for the 40 buildings is shown in Fig. 2 a). Note that no significant dependency or correlation between  $W$  and  $B$  variables are observed from the whole database (Fig. 2 a). To further investigate a possible dependency between building weight and breadth, subsets corresponding to 1, 2 and 3-story buildings were analysed. Although no clear correlation was observed for the 1 and 3-story building sets, e.g. Fig. 2 c), a positive correlation was noted for the 2-story building sets (Fig. 2 b) and d)). The correlation coefficient,  $r$ , for the 2-story buildings, is  $0.15 \cdot 0.5 = 0.39$ . Therefore,  $W$  and  $B$ , are not necessarily independent random variables, i.e.  $r \neq 0$ . Moreover, the correlation between  $\log(W)$  and  $\log(B)$  is larger than the one observed for the direct variables, as can be seen from Fig. 2 d), where a coefficient  $r = 0.247 \cdot 0.5 = 0.50$  is obtained. It is considered that this correlation between  $W$  and  $B$  for the 2-story buildings is due to local practices and also to regulations at the municipality level, which standardize the maximum number of stories for a given building breadth.

The probability distribution of the ratio of building weight and width,  $W/B$ , where the two variables are correlated, is calculated thus (Hinkley, 1969; Cogollo 2017, personal communication):

$$f\left(Z = \frac{W}{B}\right) = \int_{-\infty}^{+\infty} |B| g(W = ZB, B) dB \quad (8)$$

where the joint, bivariate, density function  $g(W = ZB, B)$  has to be known. The term  $|B|$  is the absolute value of building breadth and represents the Jacobian of the transformation  $W = ZB$ . A bivariate log-normal distribution for  $g(W = ZB, B)$  characterized by medians, standard deviations of building weight and breadth, and its corresponding correlation coefficient was assumed. Therefore, the distributions obtained for  $W/B$  are also log-normal. Results of parameters that characterize distributions of  $W/B$ , after evaluating Eq. (8) numerically, are shown in Table 3 for 6 types of HAZUS buildings in the USA, and for the unreinforced masonry low-rise buildings in Colombia, URML-COL. HAZUS-USA types of buildings used were W1 (wood, light frame), W2 (wood, commercial and industrial), C2L (concrete shear walls, low-rise), C2M (concrete shear walls, medium-rise), C2H (concrete shear walls, high-rise), URML (unreinforced masonry bearing walls, low-rise). Weights and breadths parameters for the USA buildings were estimated from Kircher (2012a, 2012b), while those for Colombian buildings were calculated from the database described before (Fig. 2).

### 3.2.2. Lateral capacity parameters ( $A_U$ , $A_y$ )

Mean and median values of building strength,  $A_U$  or  $A_y$ , and also their variability are taken from HAZUS tables, for the USA buildings. The standard deviation nat-log,  $\sigma_{\ln(A_U \text{ or } A_y)}$  is therefore 0.3 for Pre-Code and 0.25 for Code designed buildings. In order to know parameters values for other regions, e.g. Colombia, a case study was done using the same database of unreinforced masonry buildings utilized for the city of Medellin, which was described in the  $W/B$  parameter section above.

URML Buildings in the Colombia dataset have an average wall thickness of 20 cm. To determine buildings strength, we executed an analysis of the in-plane of wall resistance (wall resistance parallel to acting debris flow forces) following the procedures given in Acevedo et al. (2016) and Acevedo and Jaramillo (2015). These authors used deterministic methods provided by Borzi et al. (2008) and Benedetti and Petrini (1984), which model buildings behaviour using simplified pushover curves. Main variables needed are building heights, wall density (wall area over floor area ratio), slab weight over floor area ratio, dead load, masonry shear resistance, weights and wall thicknesses (Acevedo and Jaramillo, 2015). Buildings variables can be obtained directly from field measurement, drawings or aerial and satellite photographs. Monte Carlo simulations, using mean values and uncertainties calculated from the dataset, are utilized to handling the random variables and obtaining pushover curves and their characteristic parameters. Fig. 3 provides the in-plane pushover curve for each one of the simulated buildings as well as the mean curve (darker line) in which  $A_U = 0.53 g$  was obtained. As regards the uncertainty, a nat-log,  $\sigma_{\ln(A_U \text{ or } A_y)}$ , of 0.33, extracted from the simulations for Colombia buildings was used.

The modal mass parameter,  $\alpha_1$ , is taken as 0.90, for URML buildings following Priestley et al. (2007). The  $\lambda$  parameter is considered to take the same values provided by HAZUS.

## 4. Debris flow fragility functions

Fragility curves were calculated using both Monte Carlo simulation and a direct approach. The direct approach assumes that all random variables involved are independent log-normally distributed. Therefore, the mean of the nat-log of the resistant momentum flux for each damage state is calculated taking the logarithms to both sides of Eqs. (5), (6) and (7), and using the mean of the nat-log of every random variable. This is equivalent to evaluate the medians of momentum flux using the medians of each random variable directly in Eqs. (5) to (7). Standard deviations of the nat-log of the variable,  $\beta$ , are calculated using the square-root-sum-of-the-squares (SRSS) method. Note that the ratio  $W/B$

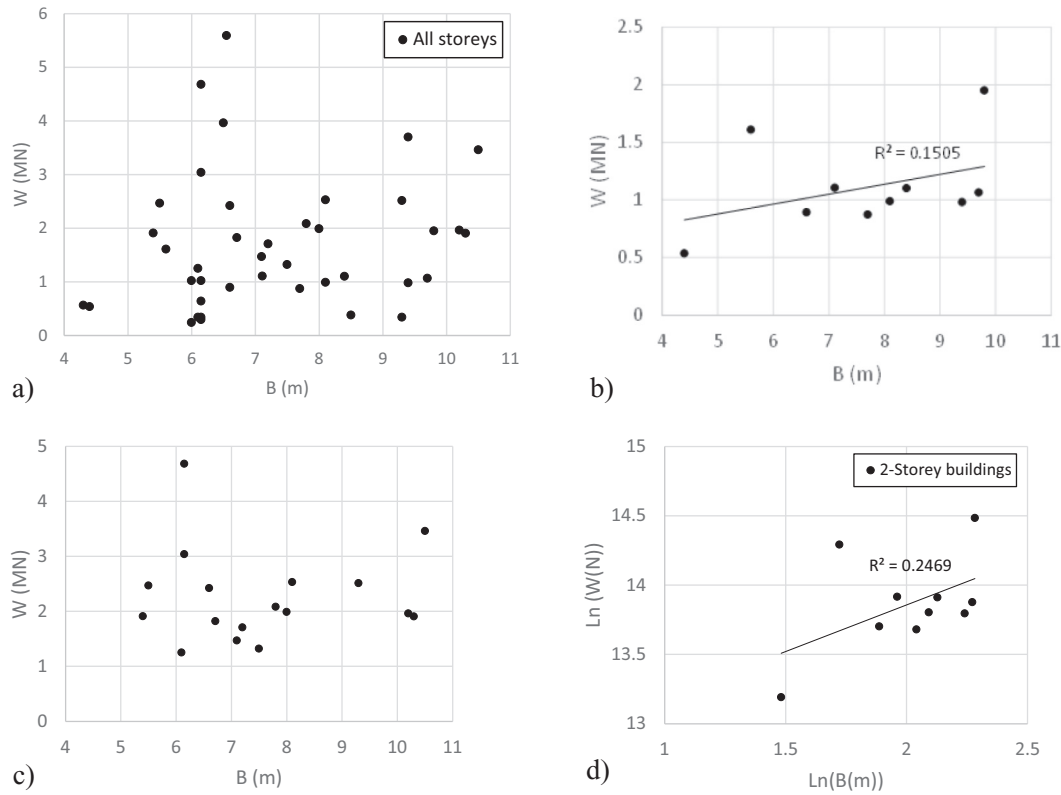


**Fig. 2.** Unreinforced masonry (URM) building dataset from Antioquia, Colombia, used for analysing correlations between building weight,  $W$ , and width,  $B$ . A positive correlation was observed for the 2-story building dataset.

**Table 3**

Input and log-normal parameters obtained for the  $W/B$  distributions. Note that for buildings other than URML in Colombia, independence of weight and breadth were assumed (then zero correlation coefficient).

Building type	$\bar{W}$ (N)	$\sigma \ln W$	$\bar{B}$ (m)	$\sigma \ln B$	Corr = $r(\ln)$	$\bar{\ln}(W/B)$	$\sigma \ln W/B$
W1	213,514.6	0.300	12.2	0.460	0	9.83	0.549
W2	889,644.3	0.300	15.2	0.460	0	11.04	0.549
C2L	8,006,798.9	0.300	21.3	0.460	0	12.90	0.549
C2M	44,482,216.0	0.300	30.5	0.460	0	14.25	0.549
C2H	106,757,318.4	0.300	30.5	0.460	0	15.11	0.549
URML	8,006,798.9	0.300	21.3	0.460	0	12.90	0.549
URML COL	812,793.2	0.604	7.1	0.243	0.5	11.52	0.527

$B$  is considered as one random variable with parameters obtained as described above (Table 3). Essentially no difference was observed between results produced by Monte Carlo simulation and the direct approach.

Examples of fragility curves were calculated for 6 representative building types from the HAZUS taxonomy. These include light frame wood structures under 460 m<sup>2</sup> (W1), commercial and industrial wood frame structures over 460 m<sup>2</sup> (W2), concrete shear wall low-rise (C2L), structures mid-rise (C2M) and high-rise (C2H) structures, unreinforced masonry bearing wall structures that are common in North America (URML), and unreinforced masonry buildings that are more common in Colombia (URML-COL). Parameters of the momentum flux ( $h v^2$ ) distributions are provided in Tables 4 to 7, while fragility curves are shown in Figs. 4 to 6. For the URML buildings in Colombia, parameters were calculated for complete damage only. This is because the simplified bi-linear pushover curves models utilized (Fig. 3) have the same ultimate ( $A_U$ ) and yield ( $A_Y$ ) strengths, so there is no difference between moderate, extensive and complete damage (the building becomes either damaged or not). More elaborate models are possible, but this is beyond of the purpose of this research.

The probability of reaching or exceeding a given damage state for a

given momentum flux is straightforward calculated as:

$$P = \Phi \left[ \frac{1}{\beta} \ln \left( \frac{h v^2}{h v_M^2} \right) \right] \quad (9)$$

Where  $\beta$  is the standard deviation of the nat-log of the momentum flux for the damage state,  $h v_M^2$  is the median, resistant, momentum flux, and  $\Phi$  is the standard normal cumulative distribution function. An interpretation of the models results shown in Tables 4 to 7 and in the fragility curves plots is that for example, URML buildings in the USA start moderate damage at a momentum flux of 18 m<sup>3</sup>/s<sup>2</sup> and complete damage at 37 m<sup>3</sup>/s<sup>2</sup>. A fairly resistant concrete shear walls, C2L, building designed according to a moderate code would start moderate damage at 28 m<sup>3</sup>/s<sup>2</sup> and complete damage from 70 m<sup>3</sup>/s<sup>2</sup>. Wooden buildings, 1 to 2 storey, common in the USA, designed according to moderate code, would start moderate damage at a low 2 m<sup>3</sup>/s<sup>2</sup> and will sustain complete damage from 6 m<sup>3</sup>/s<sup>2</sup>. In Colombia, URML buildings, the most common type in the region of Antioquia, and Colombia itself, will suffer complete damage at a threshold of 23 m<sup>3</sup>/s<sup>2</sup>. Probabilities of being in each damage state knowing a hazard level are easily calculated from Eq. (9).

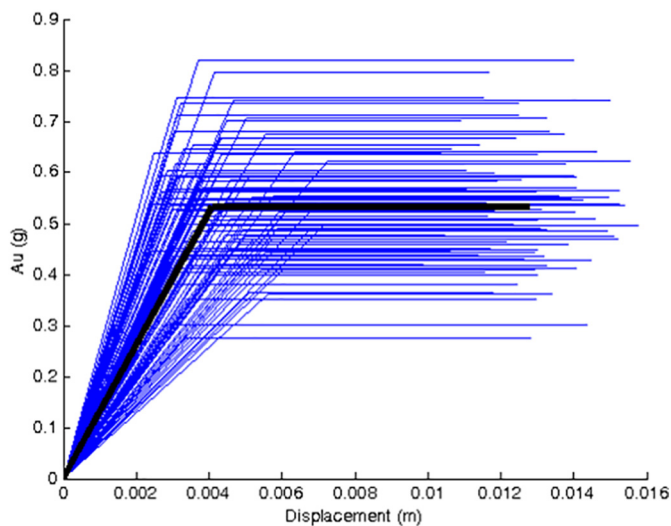


**Fig. 3.** Pushover curve for the in-plane resistance for URML, 20 cm thick wall, buildings in Antioquia, Colombia. Note that an average  $A_U$  strength of 0.53 g (black full line), is obtained for in-plane resistance.

**Table 4**

Fragility curve parameters, USA pre-code, and Colombia URML buildings. Note that for the Colombia buildings, parameters for complete damage only are provided because of the model used, as explained in the text.

Pre code and Colombia URML buildings						
Type	Moderate		Extensive		Complete	
	Median	$\beta$	Median	$\beta$	Median	$\beta$
	$(hv^2)$ $m^3/s^2$	sdln	$(hv^2)$ $m^3/s^2$	sdln	$(hv^2)$ $m^3/s^2$	sdln
W1	1.37	0.902	2.75	0.90	4.12	0.90
W2	2.29	0.902	4.00	0.90	5.72	0.90
C2L	14.78	0.902	25.86	0.90	36.94	0.90
C2M	47.47	0.902	83.22	0.90	118.97	0.90
C2H	67.87	0.902	119.57	0.90	171.28	0.90
URML	19.70	0.902	29.55	0.90	39.40	0.90
URML-Col, in plane $A_U = 0.53$ g					23.39	0.90

**Table 5**

Fragility curve parameters, USA, low code.

Low code						
Type	Moderate		Extensive		Complete	
	Median	$\beta$	Median	$\beta$	Median	$\beta$
	$(hv^2)$ $m^3/s^2$	sdln	$(hv^2)$ $m^3/s^2$	sdln	$(hv^2)$ $m^3/s^2$	sdln
W1	1.40	0.89	2.79	0.89	4.19	0.89
W2	2.33	0.89	4.07	0.89	5.82	0.89
C2L	15.03	0.91	25.94	0.89	37.57	0.89
C2M	48.28	0.89	84.64	0.89	120.99	0.89
C2H	74.77	0.89	131.74	0.89	188.71	0.89
URML	19.76	0.90	29.64	0.90	39.53	0.90

## 5. Model validation

In order to highlight the consistency of the method described before a comparison of model results with those from field data obtained in South Korea is presented below. The analogy will include: damage field data for general URML buildings compiled during several debris flow

**Table 6**

Fragility curve parameters, USA, moderate code.

Moderate code						
Type	Moderate		Extensive		Complete	
	Median	$\beta$	Median	$\beta$	Median	$\beta$
	$(hv^2)$ $m^3/s^2$	sdln	$(hv^2)$ $m^3/s^2$	sdln	$(hv^2)$ $m^3/s^2$	sdln
W1	2.09	0.89	4.19	0.89	6.28	0.89
W2	4.65	0.89	8.14	0.89	11.63	0.89
C2L	30.05	0.89	52.60	0.89	75.14	0.89
C2M	97.14	0.89	169.86	0.89	242.57	0.89
C2H	150.73	0.89	263.48	0.89	376.24	0.89

**Table 7**

Fragility curve parameters, USA, high code.

Moderate code						
Type	Moderate		Extensive		Complete	
	Median	$\beta$	Median	$\beta$	Median	$\beta$
	$(hv^2)$ $m^3/s^2$	sdln	$(hv^2)$ $m^3/s^2$	sdln	$(hv^2)$ $m^3/s^2$	sdln
W1	2.79	0.89	5.59	0.89	8.38	0.89
W2	9.31	0.89	16.29	0.89	23.27	0.89
C2L	60.11	0.89	105.19	0.89	150.27	0.89
C2M	193.70	0.89	339.13	0.89	484.55	0.89
C2H	290.78	0.89	522.22	0.89	753.66	0.89

Fragility curves for the USA, moderate-code, and for Colombia URML buildings are plotted in Figs. 4–6.

events in Korea (Kang and Kim, 2016), fragility curves developed utilizing the model described here using structural data from a specific URML building type in Korea (Yi et al., 2004), and the modelled fragility curves for URML buildings in Colombia that was presented above.

A main shortcoming in the process of testing debris flow fragility models is the scarcity of published data that provide both pieces of main parameters needed, i.e. hazard levels (depths and velocities) and reliable structural types of buildings. The 68 worldwide event dataset compiled by Jakob et al. (2012) provides hazard parameters, i.e. depth, velocities, minimum, average and maximum momentum flux, but no structural characteristic of buildings, that allows a classification using the HAZUS system, for example, are included. A dataset that includes hazard parameters and also more specific structural data is given by Kang and Kim (2016). These authors used data surveyed and investigated in detail from 25 buildings damaged in 11 events in Korea. They provided flow depths, velocity and impact pressure at the buildings sites. At the same time, they classified buildings type and also damage states for each building following the HAZUS system. We calculated momentum flux from depth and velocity data reported by Kang and Kim (2016). Results for URML buildings, the most abundant data (a group of 8 URML buildings that reached complete damage), are shown in Table 8.

The approximate cumulative distribution, using rank statistics (taking the values of momentum flux, ordered from the highest to the lowest one, last column in Table 8, and dividing them by the total number of values to obtain the corresponding probabilities), for the 8 URML buildings within the same damage state, complete, is shown in Fig. 7 (dots). A log-normal distribution, fragility curve, can be easily adjusted to the field data shown in Fig. 7 using a least square procedure in the log-normal space (log-normal probability paper), for example. Results of the adjustment yield a median value of  $25.34 m^3/s^2$ , and a standard deviation of log equal to 1.19. The adjusted fragility curve is

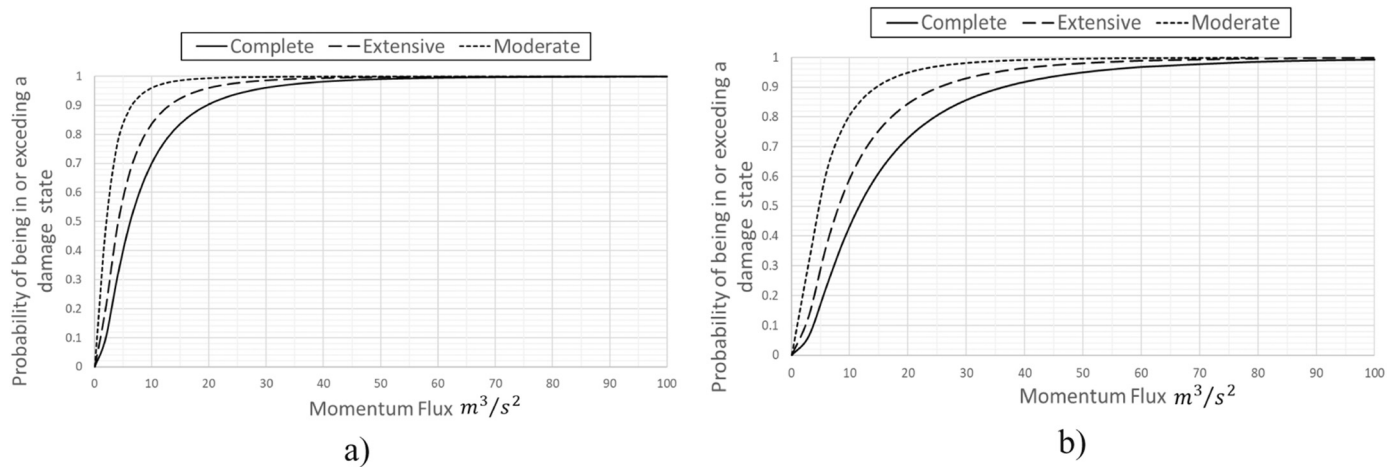


Fig. 4. Fragility curves for HAZUS wood buildings, moderate code.

also shown in Fig. 7.

The fragility curve developed using field data from Korea includes several types of buildings, which were classified as general URML structures that suffered a given damage state (Table 8). However, no specific structural details e.g. wall distributions, floor areas, floor heights, loads, etc. were provided by Kang and Kim (2016). Other researchers, Yi et al. (2004), published structural parameters for four types of URML buildings common in Korea, which are called Type A, B, C and D. These authors presented complete structural details, including a plan view drawing, of the type A building, a 6.20 m wide  $\times$  7.35 m long 2-storey structure. Therefore, and for comparison purposes, we developed a fragility curve for the type A building, for complete damage, using the Yi et al. (2004) data. A summary of structural parameters for the Type A, 2-storey URML building is shown in Table 9.

The same procedures described before, i.e. following Acevedo et al. (2016), Acevedo and Jaramillo (2015), Borzi et al. (2008) and Benedetti and Petrini (1984), were utilized for producing a simplified pushover, capacity curve, of the type A building. These procedures use building height, wall density (wall area over floor area ratio), slab weight over floor area ratio, dead load, masonry shear resistance, weights and wall thicknesses as variables. Parameters needed for generating the capacity curve of the type A building were calculated from Yi et al. (2004) data (Table 9). They are shown in Table 10.

Using values from Table 10, an ultimate building strength,  $A_U = 0.36$  g, was obtained as a characteristic parameter of the pushover curve for the Type A, URML building in South Korea. Corresponding fragility curve parameters for complete damage state were then calculated using the model described, i.e. Eq. (5), etc. Table 11 shows a

summary of fragility curve parameters for: the South Korea type A building, the field data for several buildings in South Korea, and Colombian buildings. A graphical comparison of the respective curves is presented in Fig. 8.

Fig. 8 and Table 11 highlight a significant adjustment between fragility curves for complete damage in URML buildings obtained from field data in South Korea and those deduced with the model for both: a specific type A building also in South Korea, and for general unreinforced masonry buildings in Colombia. Median values of fragility curves are similar, i.e. in the range from 20 to 25  $\text{m}^3/\text{s}^2$ . These medians represent the thresholds at which a debris flow will start complete damage, i.e. the building resistance. The difference between the median building resistance obtained from the model for the type A structure in South Korea, i.e. 20.6  $\text{m}^3/\text{s}^2$ , and that one corresponding to several type of buildings deduced from field data in Korea, i.e. 25.3  $\text{m}^3/\text{s}^2$ , is less than 20%. Note also that the difference between the median resistance of general URML buildings in Colombia, 23.3  $\text{m}^3/\text{s}^2$ , and the median strength of general South Korean buildings, from the field, is less than 8%, a striking result. This result will be discussed in the next section.

Uncertainties, represented by the standard deviations of the logarithms, are also within a reasonable range, i.e. between 1.19 for South Korea field data, compared with 0.90 for the model in Colombia and also for the specific type A building in South Korea. Although a standard deviation of the log equal to 1.19 seems to be a bit high, this uncertainty includes the statistical fact that for small samples (8 values in this case), approximate cumulative distributions decrease the probabilities associated to the highest values of the random variable artificially (The order number used for ranking statistics is divided not just

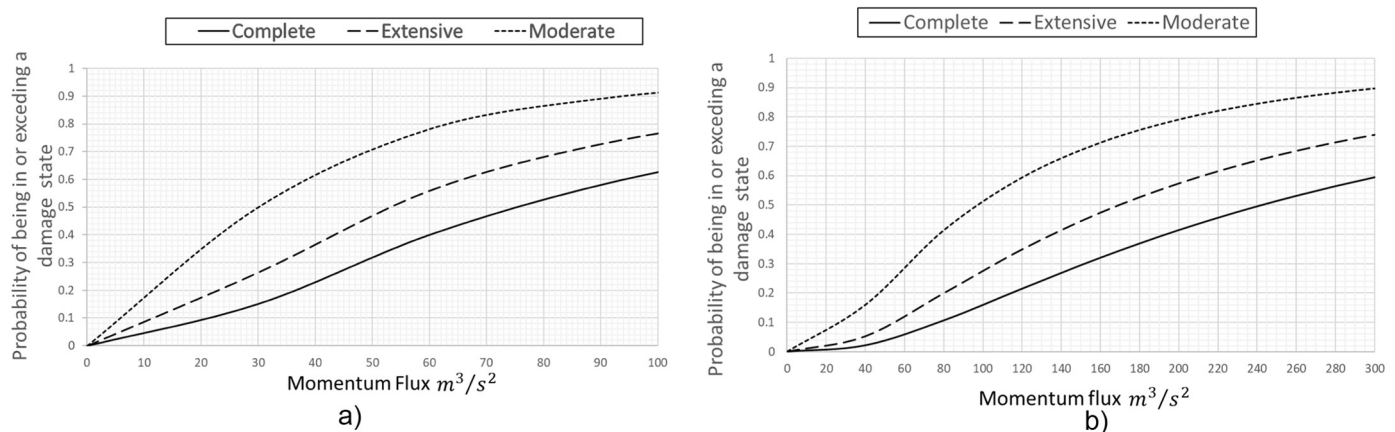


Fig. 5. Fragility curves for HAZUS Concrete Shear Walls buildings, Moderate code.

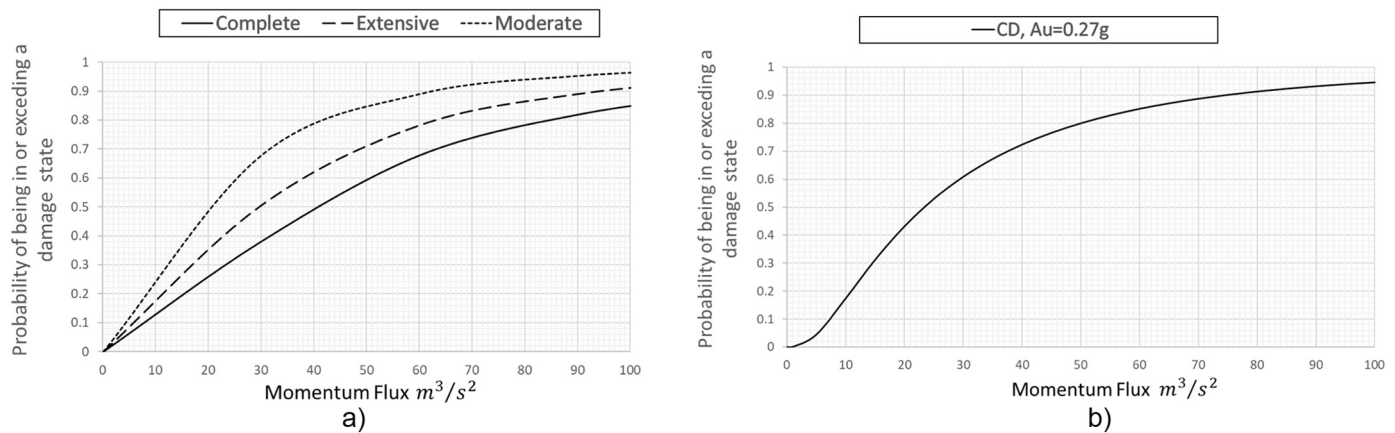


Fig. 6. Fragility curves for HAZUS and Colombian unreinforced masonry bearing walls buildings, low and pre code.

Table 8

Buildings affected by debris flow in Korea. Data from Kang and Kim (2016). Momentum flux, last column, was calculated from depth and velocity provided by these authors.

Building N°	Flow depth [d(m)]	Flow velocity [v(m/s)]	HAZUS label	Damage state	Moment flux [ $m^3/s^2$ ]
j-1	3.23	6.60	URML	Complete	140.70
i-1	3.22	4.20	URML	Complete	56.80
b-1	2.70	3.50	URML	Complete	33.08
i-2	1.98	3.70	URML	Complete	27.11
i-3	1.44	3.50	URML	Complete	17.64
a-1	1.33	3.40	URML	Complete	15.37
a-4	0.99	3.50	URML	Complete	12.13
k-1	0.71	3.20	URML	Complete	7.27
b-2	0.52	2.40	URML	Extensive	3.00
i-5	1.44	2.30	URML	Moderate	7.62
i-4	0.66	1.00	URML	Slight	0.66

by the number of values in the sample,  $n$ , but for  $n + 1$ ). That is to say, ranking statistics increases artificially the uncertainty for allowing the fact that a sample is small. Should the sample be larger, this effect would be less important, and the uncertainty from scarcity of data would be smaller. Another factor that may increase the uncertainty in the fragility curve developed for field data is the fact that URML

buildings in Korea are not composed from just one structural type but a number of them. Yi et al. (2004) identified at least 4 sub-types of URML buildings, as was already mentioned.

Further evidence of the consistency of the models described can also be taken from Jakob et al. (2012) database. In 1985, the Nevado del Ruiz volcano in central Colombia erupted producing a mudflow that

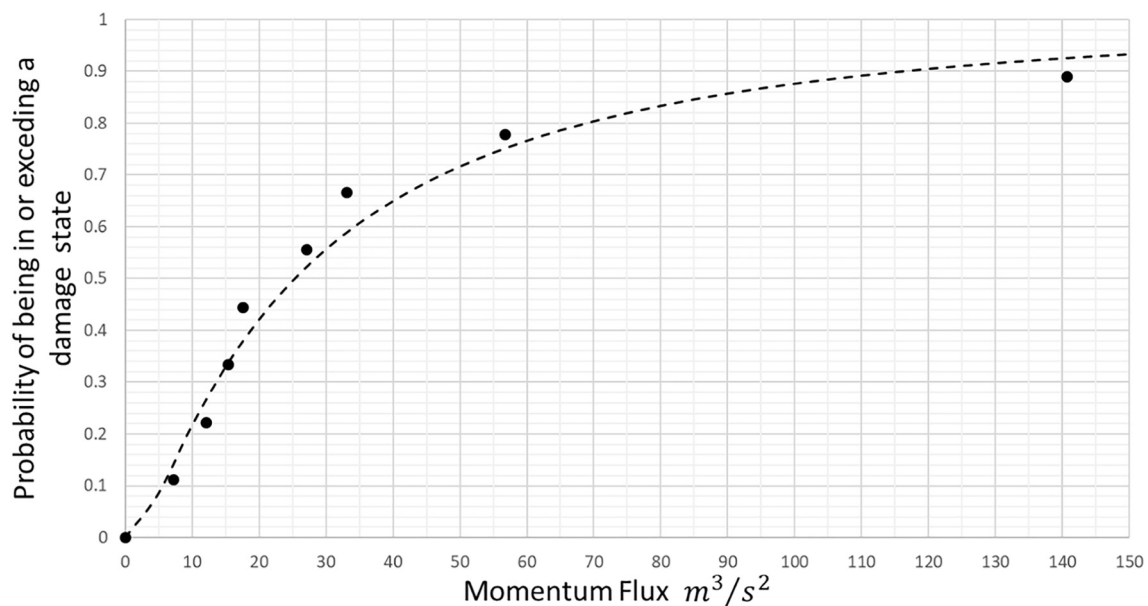


Fig. 7. Cumulative distribution of field data for 8 URML buildings in complete damage in Korea. Plot using data from Kang and Kim (2016). Dots are the field data. Adjusted log-normal fragility curve is the dashed line. A median =  $25.34 m^3/s^2$ , and a  $oln = 1.19$  for the adjusted curve are obtained.

**Table 9**

Main structural parameters of a Type A, 2-storey, URML building in Korea. Adapted from Yi et al. (2004). Slab weight was deduced from the other data provided by original authors.

Typical length, m	Typical breadth, m	Typical floor area, m <sup>2</sup>	Gross area of walls, m <sup>2</sup>	Self weight of walls, kN	Vertical axial stress on base of wall, 1st floor, kPa	Total building weight, kN
7.35	6.20	38.83	4.34	264.89	204.53	887.64

**Table 10**

Type A URML building parameters for producing the push over curve. Calculated from Yi et al. (2004).

Slab weight/floor area, kPa	Interstory height, m	Masonry shear resistance, kPa	Wall density, direction 1, m <sup>2</sup> /m <sup>2</sup>	Wall density, direction 2, m <sup>2</sup> /m <sup>2</sup>	Weight/breadth, N/m
2.32	2.70	196.20	0.066	0.059	143,314

**Table 11**

Summary parameters for fragility curves, complete damage, URML buildings.

Summary table		
Type	Median	$\beta$
	m <sup>3</sup> /s <sup>2</sup>	sdln
Korea field data	25.34	1.187
URML Colombia, in plane	23.32	0.899
URML, Type A, Korea	20.58	0.899

destroyed the town of Armero, a zone where unreinforced masonry buildings were the most common, as in many other places of Colombia. Buildings in a large part of the city were totally destroyed or washed away (Montero-Olarte, 2007). Lack of lateral strength in buildings was, and still is, frequent in Colombia because the first earthquake Code was implemented from 1984, after the 1983, Popayán, earthquake. Average momentum flux reported by Jakob et al. (2012) in Armero town is 20 m<sup>3</sup>/s<sup>2</sup>, a value that is consistent with the thresholds obtained here for complete damage state in URML buildings in Colombia.

## 6. Discussion

The method presented incorporates geological variables, i.e. density,  $\rho$ ; building performance (structural) parameters, e.g. the yield or ultimate building capacity,  $A_y$ ,  $A_u$ , the weight over breadth ratio,  $W/B$ ; and geo-structural variables, i.e. drag coefficient,  $C_d$ , debris impact coefficient,  $K_d$ , to produce fragility functions expressed in terms of momentum flux,  $h\nu^2$ . Dependency of momentum flux thresholds needed to cause a damage state, i.e. median values (median strength), on geological and structural parameters are given by Eqs. (5) to (7). To appreciate the effect of each variable in the median resistant momentum flux given by fragility curves, a sensitivity analysis was executed for the case of complete damage for URML buildings in Colombia, where a threshold value of 23.3 m<sup>3</sup>/s<sup>2</sup> was calculated from the model. The analysis was done, using a Monte Carlo simulation, i.e., allowing the parameter under study change freely according to its probabilistic

distribution while keeping fixed the other variables at their mean values and recording the range of momentum flux obtained. Results are presented in Table 12.

Results from Table 12 highlights that the parameters that produce higher variability, i.e. large uncertainty, in the predicted median momentum of fragility curves are the weight over breadth ratio,  $W/B$ , and the impact coefficient,  $K_d$ , (both parameters produce momentum flux range between 10 and 60 m<sup>3</sup>/s<sup>2</sup>). This result is not surprising when the uncertainties, measured by the standard deviations of the individual parameters, are examined (Column 3, Table 12). Both  $W/B$  and  $K_d$  have the highest uncertainty in the model (0.53). Therefore, it is worth remaining that the higher the level of uncertainty of a variable, the more influence it has in the general uncertainty of the model. The high uncertainty value for the  $W/B$  ratio comes from the fact that a portfolio of buildings, rather than specific structures, has been used for the model. Using parameters obtained from portfolios is a practical choice for general risk studies. However, for analysis of damage and losses to individual buildings, specific variables obtained through inspections, drafts reviews, analysis of photographs, etc., should be used, which produces an automatic reduction in the uncertainty of structural parameters (including also the  $A_u$  parameter), and therefore, in the variability of values estimated by the model.

The impact parameter,  $K_d$ , represents the effect of coarse particles (and any type of coarse solid debris) in a hydraulic model. Note that for a mean value of 2 for the drag coefficient,  $C_d$ , (used in our model) Eq. (1) becomes  $F_{DF} = K_d \rho B (h\nu^2)$  which has the same form as the typical thrust force expression mentioned in the literature (e.g. Hung et al., 1984; Bugnion et al., 2012; Scheidl et al., 2013; Ch et al., 2015; Zhang et al., 2016; Vagnon and Segalini, 2016). Values for the impact coefficient reported by these authors have a large variability (0.4 to 12). However, a direct comparison between different values reported is not straightforward because distinct approaches followed for different researchers, e.g. type of hypotheses, setting of experimental tests, scaling procedures, nature of barriers (rigid, flexible), grain size distributions, single or two-phase model, mixture densities, among others. Vagnon and Segalini (2016), using the non-dimensional Froude number, have found impact parameters ranging between 0.5 and 1.2. While there is a clear need to produce uniform results of current research regarding the

**Table 12**

Sensitivity analyses of model variables, for complete damage in URML buildings in Colombia.

Parameter under analysis	Range of median momentum flux obtained (m <sup>3</sup> /s <sup>2</sup> ). (median of the whole model = 23.3 m <sup>3</sup> /s <sup>2</sup> )	Standard deviation of nat log of variable according to the model (sdln = 0.90 for the whole model)	Order of significance (influence of parameter)
$W/B$	10 to 60	0.53	1
$K_d$	9 to 60	0.52	2
$C_d$	14 to 46	0.37	3
$A_u$	13 to 44	0.33	4
$\rho$	21 to 26	0.12	5

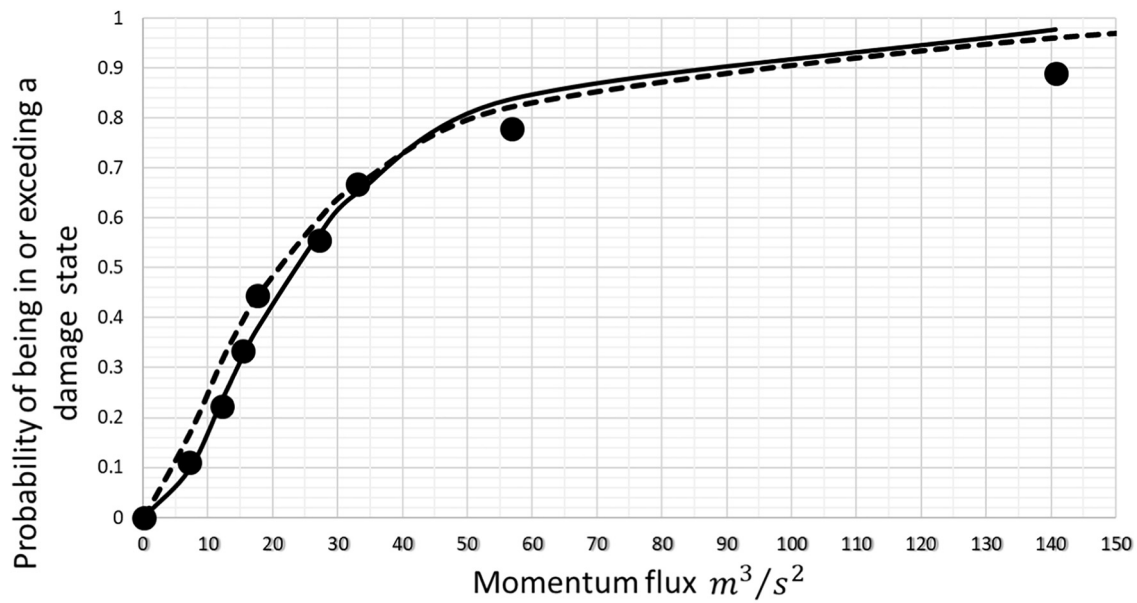


**Fig. 8.** Fragility curves for complete damage in URML buildings for the following 3 cases: Field data from South Korea (dots), Type A building in South Korea (dashed line), and Colombia buildings using the model (solid line).

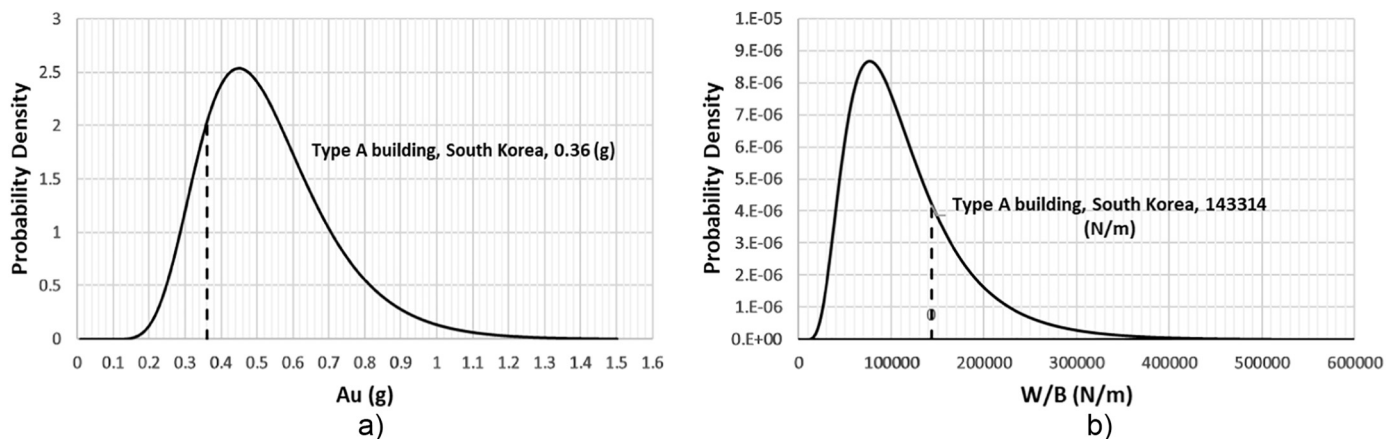


**Fig. 9.** Probability distributions of ultimate capacity,  $A_U$  and weight over breadth ratio,  $W/B$ , used by the model, including specific values of type A South Korean buildings.

impact coefficient, and also to generate more research for the case of buildings, the South Korea field data, highlighted in Fig. 8, shows that the selection of a probability distribution for the impact coefficient with a mean of 1.2 produce model results that are consistent with field evidence for the case of damage to URML buildings.

The similarity between fragility curves for URML buildings in South Korea and those in Colombia, Fig. 8, can be also explained following the main parameters that define median values for the model. The geological parameters, e.g. density and  $K_d$ , can have large variations according to grading of coarse and fine material in the debris flow, the concentration and rheological behaviour. Kang and Kim (2016) used data of 11 different events in Korea to obtain the field dataset utilized here. The use of several debris flow events, instead of just one, produces an averaging effect of the geological parameters that is translated to the fragility curve obtained from the field. This averaging is represented in the model by using the mean values of the probabilistic functions that define the geological parameters. Regarding structural parameters and its effects, it is clear that they can have significant local differences, e.g. type of masonry, wall thickness, wall distributions by floor, slabs and roofs types, floor areas, construction practices, in general different

geometrical characteristics. These parameters are used to calculate the ultimate building capacity,  $A_U$ , and the weight to breadth ratio,  $W/B$ . They are multiplicative in the process to obtain the median building strength of the fragility curve following Eq. (5). Clearly, buildings resistance to debris flows depends on both lateral strength and unit building weight. Yi et al. (2004) published structural parameters for URML buildings in South Korea, as was already presented. An ultimate capacity,  $A_U = 0.36$  g, was obtained for type A building. The average weight to breadth ratio for South Korean buildings, which can be easily calculated from Yi et al. (2004) is 190 kN/m, while the Type A building  $W/B$  ratio is 143 kN/m. On the other hand, Colombian buildings have average ultimate capacity,  $A_U = 0.53$  g, as was already presented, and average weight to breadth ratio,  $W/B = 115$  kN/m (calculated from Table 2). Fig. 9 shows the probability distributions of ultimate strength and weight to breadth ratio used by our model for Colombian buildings including the values for South Korea type A building. Note that both structural parameters for these two different geographical environments range well within the probability distributions used by the model. Also note that while Korean URML buildings are heavier (per unit length) than analogous Colombian structures, they may have less

ultimate capacity than those from Colombia. These two effects are mixed to produce a structural averaging effect, which combined with the several debris flow events, mentioned before, generates fragility curves that are similar for two different geographical regions.

Other aspect that deserves a brief comment is the hazard parameter utilized in the model, i.e. the product of debris flow deposition height times velocity squared,  $h v^2$ . This parameter has a clear physical meaning because is both the flux of momentum rate per unit mass of debris, i.e. the flux of force per unit mass, and also the debris discharge rate, i.e. the slope of a debris flow Hydrograph. It is meaningful to associate damage to structures not just to the debris discharge but to the rate of change of it.

Results of the comparison between modelled fragility curves and those obtained from field data, which shows significant similarities, plus further field evidence, as in the case of Nevado del Ruiz, Colombia, mud flow, highlights that the method described is consistent. It is considered that equating debris flow hydrodynamic forces to buildings lateral strength and then including the randomness of the involved variables, following a similar procedure as the one used for tsunamis, is a rational and simple approach to produce fragility curves for debris flows.

### 6.1. Limitations

The interaction between debris flows and structures is a complex phenomenon. A number of geological variables e.g. origin, grain-size distribution, viscosity, density, water content, etc., interact with structural properties, e.g. wall distributions, materials properties, storey height, general building geometry, etc. The method described for calculating fragility curves is a general framework that averages basic geological and structural parameters, and do not attempt representing an exact and very specific building behaviour subjected to a particular debris flow. Real field behaviour may deviate of average values given by the model. Therefore, it is considered that the model proposed works better for risk analyses in portfolios and regional studies than for analyses for individual buildings and very specific geological conditions. In particular, detailed building design against debris flow hazards has to wait until more field data become available and knowledge on the physics of the fluid-building interaction increases. Other approaches to the vulnerability against debris flow hazard problem could also be useful, e.g. Mazzorana et al. (2014).

The model introduced has its bases on the relation between average hydrodynamic forces and buildings strength. Therefore, it includes only the parameters provided in a hydraulic model formula and those ones in the general lateral strength of buildings, Eqs. (1) to (7). All parameters needed by the model can be obtained either from field data, e.g.  $W/B$  ratio,  $A_u$ , density, or from values proposed here, e.g.  $K_d$  and  $C_d$ , which adjust well to field observations. Future data will improve accuracy of the model. Also note that the effects of erosion, or complex processes like remobilization and/or re-deposition, which can affect the hazard level, are excluded from the method presented.

It is important remembering that the procedure described is consistent and seems to work well for the case of complete damage to unreinforced masonry low rise, URML, buildings. Debris flow fragility curves for other type of buildings, e.g. wooden, reinforced concrete frames, etc, have been provided or can be easily calculated with the model. Results from these calculations can be used as sources of preliminary estimations for risk analyses, but more accurate estimations have to wait until further research is available. In particular, the effect of debris flows on intermediate to high rise buildings is an open issue for investigation. In addition, the expected building damage described by the models assumes that the main direction of debris flow is perpendicular to the buildings, but do not says too much of cases where the attack angle is less than  $90^\circ$ . In those cases, Eq. (1) has to be multiplied by the sine of the least angle between the building main wall and the

direction of the debris flow. This effect has to be investigated in the future. Other issues to be investigated in more detail are the mean values and uncertainties of the impact coefficient, as was already said, especially the effect of big single blocks and constructions where the building is supported by skeleton of bars and pilots.

The model proposed is being shown to be consistent for complete damage state, for which there are more field data available in the literature than for lower damage state levels. Less is said about other damage states, e.g. moderate. It is also possible that lower than complete damage is related to out-of-plane failure in walls (wall resistance perpendicular to acting debris flow forces) and material intrusions effects, for example. These issues have to be further investigated.

Similarities between debris flow fragility curves obtained for different geographical regions are found just for Colombian and Korean URML buildings. Note, for example, that results from the model yields median resistance for URML buildings in the USA in the order of  $39.40 \text{ m}^3/\text{s}^2$ , whereas for Colombia and Korea are in the order of  $24 \text{ m}^3/\text{s}^2$ . Clearly, specific analyses should be done for every region.

## 7. Conclusions

A method to produce building fragility curves for debris flows using the flux of momentum rate per unit mass, i.e. the debris discharge rate, as a hazard parameter has been presented. Fragility curves, rather than vulnerability functions, are needed because they: allow direct calculation of probabilities of casualties, can be used in state-of-the-art methods for engineering design, include the effects of main uncertainties, and facilitate the calculation of damage probabilities due to multiple hazards.

The method equates the debris flow hydrodynamic force to the building lateral strength, building capacity, and then includes the randomness of variables involved, similarly to the procedure utilized for tsunamis. Parameters needed are debris flow density,  $\rho$ , drag coefficient,  $C_d$ , debris impact coefficient,  $K_d$ , yield and ultimate building capacity,  $A_y$  and  $A_u$ , and the building weight to breadth ratio,  $W/B$ . These parameters are considered statistically independent. Nevertheless, to obtain the distribution of the weight to breadth ratio, an analysis of a possible correlation between building weight and breadth is recommended. This type of correlation could arise due to local regulations and construction practices.

A comparison of results between fragility curves for complete damage in URML buildings developed using this model plus one obtained from field data in Korea, in combination with further field evidence in Colombia shows that the method is consistent. It was also found that fragility curves for two different geographical regions could be similar due to the average interaction of the parameters involved. For example, the median discharge rate needed to produce complete damage in URML buildings in both Korea and Colombia is on the order of  $24 \text{ m}^3/\text{s}^2$ . However, this similarity is not universal, and specific fragility curves for the same type of buildings in different regions must be developed.

It is considered that the procedures described are consistent, rational and simple. Nevertheless, care should be exercised when using results of the model for materials other than masonry, especially in the case of high rise buildings. Specific analyses should be done for those cases where the main debris flow direction is not perpendicular to buildings walls.

The uncertainties involved and averaging methods makes the proposed model suitable for risk analyses of portfolios. More specific studies should be attempted with care. In particular, investigations of the impact coefficients must be executed.

Fragility curve parameters in terms of momentum flux are significant tools for mitigation purposes. On one hand, median values provide the threshold at which damage starts, so they can be used for debris flow hazard zonation maps. These hazard maps can be drawn specifically, for each building type, which is a useful tool for urban planning and regulation policies. On the other hand, the full probability

distribution of momentum flux can be used to calculate expected losses in any debris flow risk study.

## Acknowledgments

We wish to express our gratitude to: Juan H. Cadavid who offered useful insights on incorporating concepts of momentum flux, hydrodynamic forces and drag coefficients to model physical characteristics of debris flow events; Myladis Cogollo, who provided a method to obtain probability densities for the quotient of correlated random variables; Juan M. Mosquera, who provided insightful comments on building resistance; Alvaro J. Gonzalez, who gave us useful input on debris flow characteristics; Alfonso M. Ramos and William Murphy, who reviewed an earlier version of the manuscript with suggestions for revisions; and Nicky Hastings for support and encouragement. Two unknown reviewers provided useful insights to enrich the manuscript. Our appreciation and thanks to all of them.

## References

- Acevedo, A.B., Jaramillo, J.D., 2015. Development of exposure and vulnerability for Antioquia (Colombia)-South American Project. In: Global Earthquake Model, GEM. Research Report Foundation-EAFIT University (90 pp).
- Acevedo, A.B., Jaramillo, J.D., Yepes, C., Silva, C., Osorio, F.A., Villar, M., 2017. Evaluation of the seismic risk of the unreinforced masonry building stock in Antioquia, Colombia. *Nat. Hazards* 86 (Suppl 1), 31. <http://dx.doi.org/10.1007/s11069-016-2647-8>.
- Akbas, S.O., Blahut, J., Sterlacchini, S., 2009. Critical assessment of existing physical vulnerability estimation approaches for assessment of debris flows. In: Mallet, J., Rémaitre, A., Bogaard, T. (Eds.), *Landslides Processes: From Geomorphological Mapping to Dynamic Modelling*. CERIG, Editions, Strasbourg, pp. 229–233.
- Benedetti, D., Petrini, V., 1984. Sulla vulnerabilità sismica di edifici in muratura: proposta su un metodo di valutazione. *L'industria delle Costruzioni* 149, 66–74.
- Borger, P., 1999. Risikoanalyse bei gravitativen Naturgefahren. Bundesamt für Umwelt, Wald und Landschaft, Bern.
- Borzi, B., Crowley, H., Pinho, R., 2008. Simplified Pushover-Based Earthquake Loss Assessment (SP-BELA) Method for Masonry Buildings. *Int. J. Archit. Heritage* 2, 353–376.
- Bugnion, L., Mcardell, B.W., Bartelt, P., Wendeler, C., 2012. Measurements of hillslope debris flow impact pressure on obstacles. *Landslides* 9, 179–187.
- Cadavid, J. (Noviembre de 2017). J. A. Prieto, Interviewer.
- Calvo, B., Savi, F., 2009. A real world application of Monte Carlo procedure for debris flow risk assessment. *Comput. Geosci.* 25, 967–977.
- Cascini, L., Cuomo, S., Pastor, M., Rendina, I., 2016. SPH-FDM propagation and pore water pressure modelling for debris flows in flume tests. *Eng. Geol.* 213, 74–83.
- Ch, Zeng, Peng, C., Zhiman, S., Lei, Y., Chen, R., 2015. Failure modes of reinforced concrete columns of buildings under debris flow impact. *Landslides* 12, 561–571.
- Cogollo, M. R. (June 2017). J. A. Prieto, Interviewer.
- Denlinger, R.P., Iverson, R.M., 2001. Flow of variably fluidized granular masses across three-dimensional terrain 2. Numerical predictions and experimental test. *Rev. Geophys.* 106, 553–566.
- Dowling, C.A., Santi, P.M., 2014. Debris flows and their toll on human life: a global analysis of debris-flow fatality from 1950–2011. *Nat. Hazards* 71, 203–227.
- FEMA, 2008. Guidelines for design of structures for vertical evacuation from tsunamis. In: FEMA P646, (June).
- FEMA, 2012. Seismic performance assessment of buildings. In: Methodology, prepared by Applied Technology Council. Vol. 1 ATC, FEMA P-58-1 (September).
- FEMA, 2017. HAZUS 4.0 software. <https://www.fema.gov/hazus-modernization> (last accessed 15 July 2017).
- Freeman, S.A., 1998. Development and use of capacity spectrum method. In: VI US National Conference on Earthquake Engineering, Seattle, pp. 12 AB-2. (12pp).
- Fuchs, S., Heiss, K., Hübl, J., 2007. Towards an empirical vulnerability function for use in debris flow risk assessment. *Nat. Hazards Earth Syst. Sci.* 7, 495–506.
- Haugen, E.D., Kaynia, A.M., 2008. Vulnerability of structures impacted by debris flow. In: Chen, Z., Zhang, J.-M., Ho, K., Wu, F.-Q., Li, Z.-K. (Eds.), *Landslides and Engineered Slopes*. Taylor & Francis, London, pp. 381–387.
- Hinkley, D.V., 1969. On the ratio of two correlated normal random variables. *Biometrika* 56 (3), 635–639.
- Hungr, O., McDougall, S., 2009. Two numerical models for landslide dynamic analysis. *Comput. Geosci.* 35 (5), 978–992.
- Hungr, O., Morgan, G.C., Kellerhals, R., 1984. Quantitative analysis of debris torrent hazards for design of remedial measures. *Can. Geotech. J.* 21, 663–677.
- Hutter, K., Svendsen, B., Rickenmann, D., 1996. Debris flow modeling: a review. *Contin. Mech. Thermodyn.* 8, 1–35.
- INMLCF, 2017. Instituto Nacional de Medicina Legal y Ciencias Forenses (Colombian office of the Coroner). <http://www.medicinalegal.gov.co/documents/10180/4328138/CADAVERES+IDENTIFICADOS+9+ABRIL+.pdf/0c1ed1b-6274-4b5e-b75c-cf96e95157b6> (Last accessed 15 April 2017. in Spanish).
- Iverson, R.M., 1997. The physics of debris flows. *Rev. Geophys.* 35 (3), 245–296 August.
- Iverson, R.M., 2005. Debris-flow mechanics. In: *Debris-flow Hazards and Related Phenomena*. Springer Berlin Heidelberg, Berlin, Heidelberg, pp. 105–134.
- Iverson, R.M., Denlinger, R.P., 2001. Flow of variably fluidized granular masses across three-dimensional terrain 1. Coulomb mixture theory. *J. Geophys. Res.* 106 (B1), 537–552 10 January.
- Jakob, M., Stein, D., Ulmi, M., 2012. Vulnerability of buildings to debris flow impact. *Nat. Hazards* 60 (2), 241–261.
- Jones, A.L., Kramer, S.L., Arduino, P., 2002. Estimation of uncertainty in geotechnical properties for performance based earthquake engineering. In: *PEER Report 2002/16*.
- Kang, H., Kim, Y., 2016. The physical vulnerability of different types of building structure to debris flow events. *Nat. Hazards* 80, 1475–1493.
- Kircher, Ch., 2012a. Draft tsunami TM-building-related damage/loss methods sections. In: Internal Report to the HAZUS/NIBS Tsunami Committee, (April 30).
- Kircher, Ch., 2012b. New building damage and loss methods for tsunami hazard. In: Presentation to the NIBS Earthquake Committee Meeting, San Francisco, (June 27).
- Kircher Ch, A., Nassar, A.A., Kustu, O., Holmes, W.T., 1997. Development of building damage functions for earthquake loss estimation. *Earthquake Spectra* 13 (4), 663–682.
- Lo, W.-C., Tsao, T.-C., Hsu, C.-H., 2012. Building vulnerability to debris flows in Taiwan a preliminary study. *Nat. Hazards* 64, 2107–2128 Office of the Coroner (2017).
- Mazzorana, B., Simoni, S., Scherer, C., Gens, B., Fuchs, S., Keiler, M., 2014. A physical approach on flood risk vulnerability of buildings. *Hydrol. Earth Syst. Sci.* 18, 3817–3836.
- Montero-Olarte, J., 2007. Flujo de detritos (lahares) catastróficos del volcán nevado del ruiz, Colombia, 11 de noviembre de 1985. In: Andina, P.M. (Ed.), *Movimientos en Masa en la Región Andina: Una guía para la evaluación de amenazas*. Servicio Nacional de Geología y Minería, Publicación Geológica Multinacional, pp. 4–432.
- Papathoma-Kohle, M., Keiler, M., Totschnig, R., Glade, T., 2012. Improvement of vulnerability curves using data from extreme events: debris flow event in South Tyrol. *Nat. Hazards* 64 (3), 2083–2105.
- Park, H., Cox, D.T., 2016. Probabilistic assessment of near-field tsunami hazards: inundation depth, velocity, momentum flux, arrival time and duration applied to sea-side, Oregon. *Coast. Eng.* 117, 79–86.
- Pastor, M., Stickle, M.M., Dutto, P., Mira, P., Fernandez-Merodo, J.A., Blanc, T., Sancho, S., Benítez, A.S., 2015. A viscoplastic approach to the behaviour of fluidized geomaterials with application to fast landslides. *Contin. Mech. Thermodyn.* 27, 21–47.
- Porter, K., 2017. A Beginner's Guide to Fragility, Vulnerability, and Risk. University of Colorado Boulder 101 pp. <http://spot.colorado.edu/~porterka/Porter-beginners-guide.pdf>.
- Priestley, M.J.N., Calvi, G.M., Kowalsky, M.J., 2007. Displacement-Based Seismic Design of Structures. IUSS Press, Pavia.
- Quan Luna, B., Blahut, J., van Westen, C.J., Sterlacchini, S., van Asch, T.W.J., Akbas, S.O., 2011. The application of numerical debris flow modelling for the generation of physical vulnerability curves. *Nat. Hazards Earth Syst. Sci.* 11, 2047–2060.
- Munich Re, 2017. Topics geo, natural catastrophes 2016. In: *Analyses, Assessments, Positions*, (2017 issue).
- Scheidl, C., Chiari, M., Kaitna, R., Mullegger, M., Krawutschuk, A., Zimmermann, T., Proke, D., 2013. *Surv. Geophys.* 34, 121–140.
- Shames, I.H., 1992. *Mechanics of Fluids*, 3rd edition. McGraw-Hill Inc.
- Takahashi, T., 1991. Debris Flow, IAHR-AIRH Monograph Series. A. A. Balkema.
- Takahashi, T., 2009. Mechanics based approach toward the mitigation of debris flow disasters. In: Sassa, K., Canuti, P. (Eds.), *Landslides Disaster Risk Reduction*. Springer, pp. 89–113.
- Totschnig, R., Fuchs, S., 2013. Mountain terrains: quantifying vulnerability and assessing uncertainties. *Eng. Geol.* 155, 31–44.
- Totschnig, R., Sedlacek, W., Fuchs, S., 2011. A quantitative vulnerability function for fluvial sediment transport. *Nat. Hazards* 58 (2), 681–703.
- Tsao, T.-C., Hsu, W.-K., Cheng, C.-T., Lo, W.-C., Chen, C.-Y., Chang, Y.-L., Ju, J.-P., 2010. A preliminary study of debris flow risk estimation and management in Taiwan. In: Chen, S.-C. (Ed.), *International Symposium Interpraevent in the Pacific Rim –Taipei* (26–30. April). Internationale Forschungsgesellschaft Interpraevent, Klagenfurt, pp. 930–939.
- Vagnon, F., Segalini, A., 2016. Debris flow impact estimation on a rigid barrier. *Nat. Hazards Earth Syst. Sci.* 16, 1691–1697.
- Yi, W.-H., Oh, S.-H., Lee, J.-H., 2004. Shear capacity assessment of unreinforced masonry wall. In: 13 World Conference on Earthquake Engineering, (Vancouver, paper 1698).
- Zhang, J., Guo, Z.-X., Wang, D., Qian, H., 2016. The quantitative estimation of the vulnerability of brick and concrete wall impacted by an experimental boulder. *Nat. Hazards Earth Syst. Sci.* 16, 299–309.